

# A Craniofacial Surgery Simulation Testbed

H. Delingette, G. Subsol, S. Cotin, J. Pignon

Epidaure Project

I.N.R.I.A

2004 Route des Lucioles

06902 Sophia-Antipolis BP 93, France

*E-mail: Herve.Delingette@sophia.inria.fr*

## ABSTRACT

We present a craniofacial surgery simulation testbed that makes extensively use of virtual reality techniques. The skull, skin and fat tissues are represented with simplex meshes, that are characterized with a constant vertex to vertex connectivity. Surfaces and volumes are respectively described as a three and four connected meshes. This representation is well suited for the implementation of surface deformations such as those exerted on the face skin under the action of fat tissues. Furthermore, cutting surface regions may be easily achieved due to the local nature of simplex meshes. The user proceeds by cutting skull fragments and reorganizing them with the help of a virtual hand. Fat tissue attached to both skin and skull adjusts the face shape to the reconstructed skull.

## 1 INTRODUCTION

The aim of craniofacial surgery<sup>10</sup> is to modify the shape of the skull in order to deal with accidental injuries or congenital malformations. The surgeon cuts several skull fragments and rearranges them to achieve desirable shape for the whole skull. The surgery is very tedious, often long and involves many specialists. Therefore, the surgical intervention must be thoroughly planned, in order to predict the post-operative shape of the skull and soft tissues. In most cases, surgical planning is performed with the help of two dimensional paper sketches.

With the appearance of computed tomography imagery, a significant research effort has concentrated on the achievement of truly tridimensional planning of craniofacial surgery. Vannier *et al.*<sup>9</sup> developed a system for evaluating deformities of a skull from 3D displayed images. Marsh *et al.*<sup>11</sup> adapted CAD software to simulate the surgery but modeling non polyhedral structures was quite difficult and consequently their system was difficult to handle. Craniofacial surgery simulation was pioneered by Cutting *et al.*<sup>4</sup> in 1986. They defined three main functionalities for completing a craniofacial surgery simulation:

- Cutting the skull model into several fragments.
- Handling the patches with six degrees of freedom.
- Measuring distances or angles on the skull in order to detect feature points and quantify deformations.

Brewster *et al.*<sup>2</sup> used symmetric transformations to evaluate the goodness of a reformed skull. Yasuda *et al.*<sup>19</sup> built a planning system that provided 2D surgical planning, 3D plan confirmation as well as a rough prediction of the post-operative aspect of the face. Other teams have achieved promising experiments in the field of craniofacial surgery simulation such as Satoh *et al.*<sup>12</sup> and.<sup>8</sup>

Advances in surgical planning has lead to the development of new operating room technologies. A craniofacial surgery system including real time sensing, model-to-reality registration and advanced man-machine interfaces, has been jointly developed by NYU Medical center and IBM.<sup>13</sup> Similar techniques applied to different surgical procedures has been elaborated at the hospital of Grenoble.<sup>3</sup>

In this paper, we describe a fully tridimensional craniofacial surgery simulator. Our system is characterized by several original functionalities. First, tridimensional face and skull models are extracted from CT and Cyberware images. Those geometric models optimally describe the original data since they closely approximate the shape of the face and skull but are described with a relatively small number of vertices.

The surgeon can then interactively cut and manipulate skull fragments with the help of virtual reality tools. Virtual reality techniques greatly enhance the dexterity of a user manipulating tridimensional data (see Bajura *et al.*<sup>1</sup> and Taylor<sup>13</sup>). Furthermore, it allows a surgeon to be trained or to rehearse a surgical procedure with the appropriate gesture.

Finally, our surgery simulator predicts the post-operative aspect of the patient face. The originality of our approach stems from the use of deformable surface and volumetric models in order to simulate the natural elasticity of the skin and the fat tissue of the face. The simulation techniques described in this paper are based on a new representation called "simplex mesh". those meshes are especially well-suited to render interactive deformation of complex organic models.

## 2 MODELING

The "virtual environment" where the user evolves, consists in a set of deformable surfaces or volumes. The skull as well as the face of a patient are represented with three dimensional surfaces of complex topology. In addition, we have modelled the interaction between the skin and the skull with "fat tissue". This tissue is a volumetric structure organized in layers that is attached both skull and face models. It consequently deforms the face model of a patient in response to the surgery operated on the skull. In order to provide an intuitive interface, we should be able to perform the following actions on the surface and volumetric models:

- Cutting and merging of surface fragments.
- Deformation and smoothing of surfaces.
- Creation of "fat tissue" between a region of the skull and a region of a face.
- Interaction between the fat tissue and the skin.

In order to satisfy those constraints, we use an original representation of surfaces and volumes called *simplex meshes* introduced by Delingette.<sup>7</sup> This representation authorizes local changes of connexity of a mesh, which are not possible with regular structures such as those used by Waters.<sup>18,14</sup>

Every model may be deformed under the influence of both internal or external forces, similarly to the scheme of deformable surfaces.<sup>6</sup> We formulate the deformation of surfaces and volumes with a law of motion derived from the classical mechanics theory. The external forces applied on a given model, are exerted either by another model

of different nature (interaction skin-tissue) or by the user who may help the deformation process. The internal forces constrain the models shape to stay close to a reference shape.

## 2.1 Representation of the skull and face

### 2.1.1 Definition

Among all surface representations, triangulations and regular grids are the most commonly used. Triangulated surfaces may be of complex topology and furthermore may be refined or decimated locally. But, it is rather difficult to formalize their deformation and smoothing because of the varying vertex connectivity. Regular grids, on the other hand, may be represented as B-splines, and their deformation may be easily computed. However, their connectivity cannot be locally altered and furthermore, they cannot represent surfaces of certain topology without exhibiting poles.

In our simulation tested, we represent all surface models with 2-simplex meshes that are dual of triangulations. The duality exchanges triangles into vertices, edges into edges and vertices into polygons (see Figure 1). A fundamental property of 2-simplex meshes is their constant connectivity equals to three. Therefore, at each vertex, we can define a tetrahedron, a 3-simplex, with a vertex and its three neighbors. It is important to note that even though 2-simplex meshes and triangulations are dual topologically, they are not dual geometrically. Consequently, we cannot define an isomorphism transforming a 2-simplex mesh into a triangulation. In another words, triangulations and simplex mesh are two distinct representations.

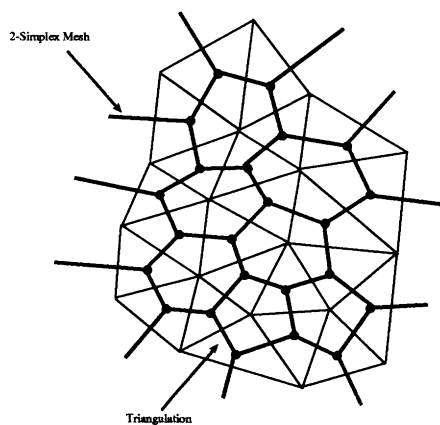


Figure 1: 2-simplex mesh and a dual triangulation.

A major advantage of simplex meshes over regular grids is their ability to perform complex mesh transformations with a small number of operations. We have defined four basic operations  $T_i^2$  ( $i = 1, \dots, 4$ ) that generate all possible transformations while keeping the 3-connexity of a 2-simplex mesh (see Figure 2). The first two  $T_1^2$  and  $T_2^2$  correspond respectively to an edge collapse and face splitting operations. Those operations modify the density of vertices and are guaranteed to keep the genus of a mesh constant.  $T_3^2$  operates on two faces and results in either the merging of two 2-simplex meshes or the creation of a handle (increase of the genus number).  $T_4^2$  consists in cutting a mesh along a contour and results in either the removal of a handle (decrease of the genus number) or the breaking a mesh into two pieces. A contour on a 2-simplex mesh is defined as a cycle of neighboring vertices. In order to perform the surgery simulation, we will use the  $T_3^2$  operation to merge skull fragments and the  $T_4^2$  operation to cut those fragments.

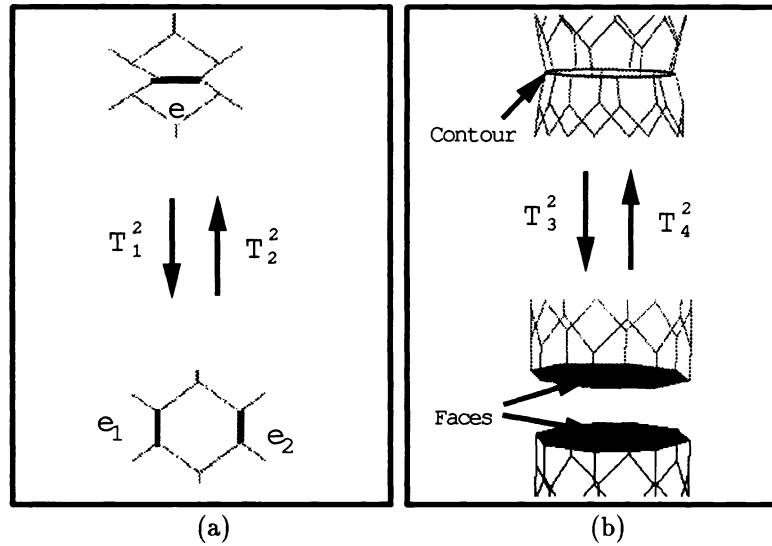


Figure 2: (a) The two Eulerian transformations  $T_1^2$  and  $T_2^2$ ; (b) the two global transformations  $T_3^2$  and  $T_4^2$  that change the mesh topology or connectivity.

### 2.1.2 Mesh Deformation

The vertices of a simplex mesh are moved under the influence of internal and external constraints. Using a mechanical analogy, we can formalize the mesh deformation with the following law of motion:

$$m \frac{d^2 P_i}{dt^2} = -\gamma \frac{dP_i}{dt} + \vec{F}_{int} + \vec{F}_{ext} \quad (1)$$

where  $m$  is the mass of a vertex and  $\gamma$  the damping factor.

Simplex meshes have a compact and non-ambiguous shape representation that makes them well-suited for deformations. At each vertex  $P_i$  of a 2-simplex mesh, we define three scalars ( $\varepsilon_i^1, \varepsilon_i^2, \varphi_i$ ) that encode the position of  $P_i$  with respect to its three neighbors. The first two parameters ( $\varepsilon_i^1, \varepsilon_i^2$ ) are *metric parameters* whereas  $\varphi_i$  is the *simplex angle* at  $P_i$ . The simplex angle is related to the discrete mean curvature  $H_i$ :

$$H_i = \frac{\sin(\varphi_i)}{\tau_i} \quad (2)$$

where  $\tau_i$  is the radius of the circumscribed triangle ( $P_{N_1(i)}, P_{N_2(i)}, P_{N_3(i)}$ ). The expression of the internal force  $\vec{F}_{int}$  is designed to control the simplex angle at  $P_i$  and consequently its mean curvature. Several expressions of the internal force are possible depending on the type of constraints we want to enforce. For instance, we will apply a shape constraint on a face model when submitted to the fat tissue actions. This constraint will ensure that the resulting face model is as close as possible to its original shape. An example of shape constraints applied on a face model is shown in figure 3. On the other hand, when merging two skull fragments, we will smooth both models to perform a realistic surgery. A detailed description of the expressions of those internal forces may be found in the technical report.<sup>5</sup>

The external forces expression include the interaction between a model and its environment. The user, for instance, may interact with a surface model with the virtual hand by exerting a repulsive force.

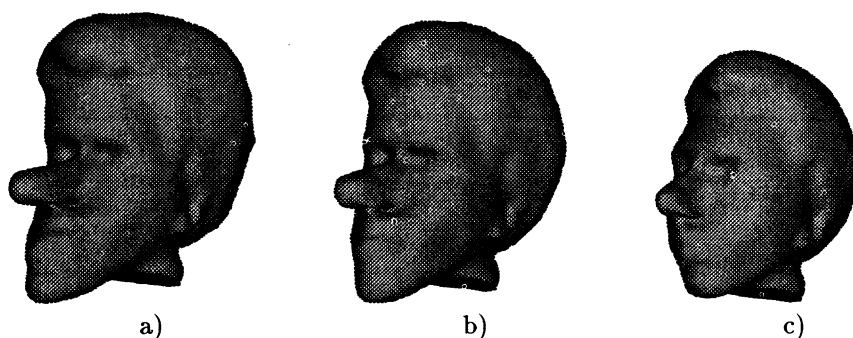


Figure 3: Shape Constraint applied on a face model; a) The initial deformed model; b) Intermediate shape; (c) Recovering its initial shape

## 2.2 Construction of the face and skull models

The extraction of the face and skull models from CT and Cyberware images is fully described in the technical report.<sup>5</sup> We proceed by deforming a generic mesh of spherical, planar or cylindrical topology in a potential field created by the edges or the isosurfaces of an image. The mesh is further refined and adapted in order to release an optimal shape description of the data. Examples of the construction of the skull and the face models are shown in figure 4 and 5.

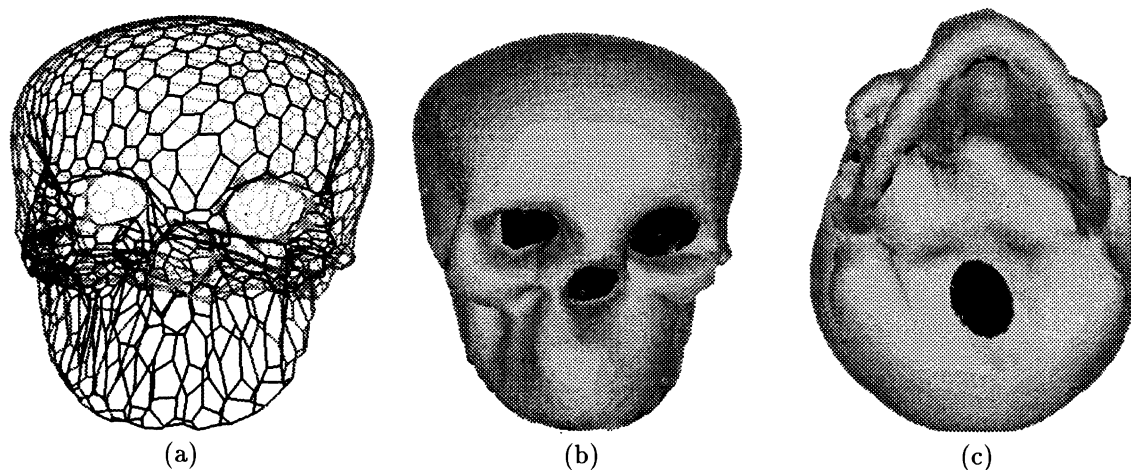


Figure 4: (a) A sphere with 2000 vertices is deformed in order to fit the skull data. The 2-simplex mesh is adapted to concentrate vertices at parts of high curvature. End contours located at the eyeballs, the nose and the foramen are automatically created; (b)(c) Front and bottom view of the rendered skull model

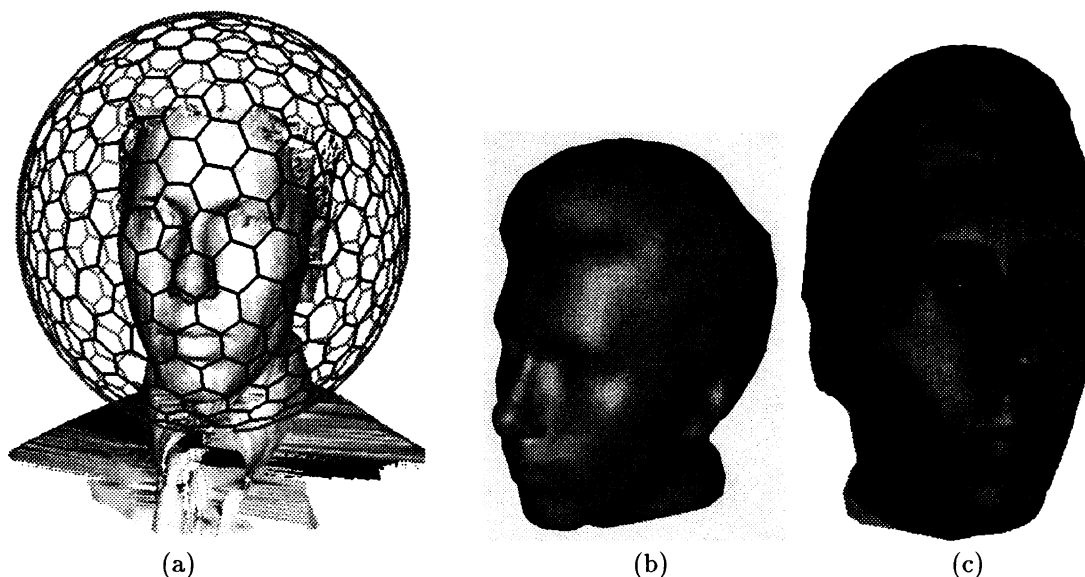


Figure 5: (a) The initial mesh with 720 vertices; (b) The rendered model of the face after refinement and adaptation of the mesh to curvature; (c) The textured face model

## 2.3 Fat Tissue Representation

### 2.3.1 Definition

Fat tissues are represented with 3-simplex meshes. A 3-simplex mesh is dual topologically of a tetrahedrisation and is characterized by a four connectivity between vertices. The combined use of 3-simplex meshes with 2-simplex meshes allows to automatically connect a region of the face and its corresponding region of the skull, with some fat tissue. We have developed an algorithm that builds a 3-simplex mesh with a prescribed number of layers between two given regions of 2-simplex meshes (see Figure 6).

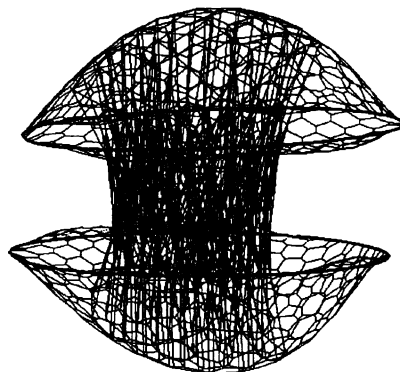


Figure 6: A 3-simplex mesh linked to two 2-simplex meshes

Consequently, we are able to vary the thickness the fat tissue layer between the skull and the face for enhancing

the realism of the face deformation. For instance, at the location of the scalp, we define a one layered 3-simplex mesh whereas between the jaw and its corresponding region on the skull, we create a three layered tissue.

### 2.3.2 Fat Tissue Elasticity

It is important to note that the deformation techniques presented in this paper are designed for surgery simulation. Therefore, the notion of fat tissue we are presenting, is different from the one introduced by Terzopoulos and Waters<sup>14</sup> or Viaud.<sup>16</sup> On the other hand, our model of face-skull interaction is similar in its concept to the work of Waters.<sup>17</sup>

Vertices of a 3-simplex mesh are moved according to the law of motion presented in equation 1. We have defined two functional modes for the fat tissue. The first mode consists in smoothing the vertices of a 3-simplex mesh such that they nicely fit between the two regions where they are anchored. The tissue has then no influence on the shape of the face. The internal force expression at a vertex belonging the tissue is then proportional to the deflection from the centroid of its four neighbors:

$$\vec{F}_{int} = \frac{(P_{N_1(i)} + P_{N_2(i)} + P_{N_3(i)} + P_{N_4(i)})}{4} - P_i \quad (3)$$

The second mode consists in exerting a force so that the tissue keeps, as much as possible, its original shape. Consequently, it induces a force on the vertices of the face, the skull model being fixed. The face model is itself constrained to keep its original shape, i.e., the shape of patient before surgery.

We then consider that a spring of rest length  $l_{ij}^0$  exists between every vertex and its four neighbors. The rest length is computed with the position of each vertices after the smoothing process. The internal force is then:

$$\vec{F}_{int} = \sum_j \frac{k_0(l_{ij} - l_{ij}^0)}{l_{ij}} \overrightarrow{P_i P_{N_j(i)}} \quad l_{ij} = \|\overrightarrow{P_i P_{N_j(i)}}\|$$

where  $k_0$  is the stiffness of the springs. We have added to the spring model, a dependency of the stiffness  $k_0$  with the elongation  $l_{ij}$  in order to model the non-linearity of the skin.

## 3 INTERACTION

### 3.1 Testbed overview

The craniofacial surgery simulation testbed has been implemented in C language on a DEC Alpha 3000/500 workstation. The user interface consists of:

- An electronic mouse for common interface functionalities.
- A virtual reality glove to interact in three dimensions with the simulation through a *virtual hand* (see Figure 7).

Two trackers Polhemus 3-Space Fastrack are fixed on the glove, one on the forefinger and the other on the thumb. They continuously measure the position and orientation in relation to an emitter box. In the simulator, geometric models and the virtual hand may be rendered, displayed in wireframe, or may be perceived in three dimensions with an anaglyph display.

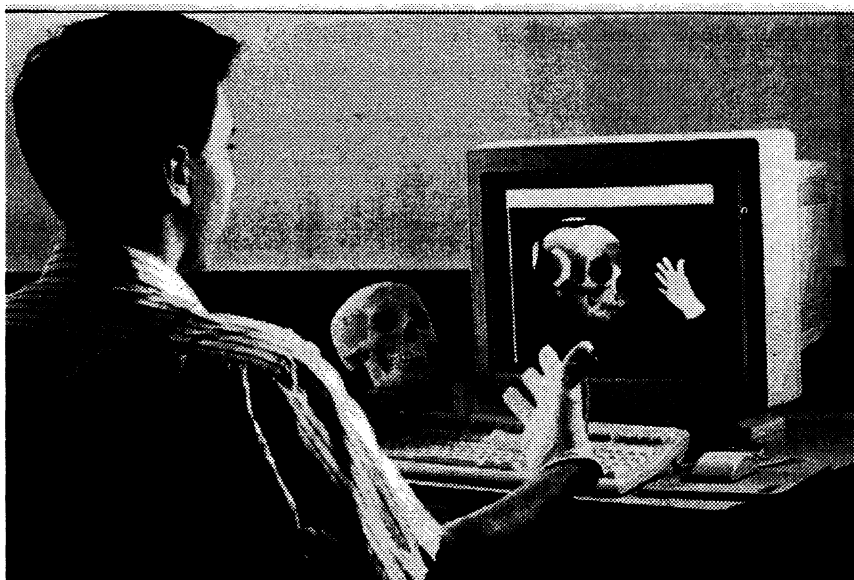


Figure 7: The craniofacial surgery simulation testbed

### 3.2 The virtual hand

Once the calibration process completed, the virtual hand follows the motion of the hand of a user, according to the translation and rotation information sent to the computer via a serial port. For each motion, the closest point in the forefinger direction of the virtual hand is computed and the object to whom it belongs is considered as pointed. When the user closes his hand, the change of distance between the two trackers is detected and the virtual hand closes and grabs the pointed object. Then, the user is able to move the object and to rotate around the hand center. Opening the hand releases the object (see Figure 8).

This pointing mode is very convenient for handling objects. But, it is too inaccurate to select a point, for instance to perform a precise cutting. Indeed, a small rotation of the hand may lead to a large displacement of the pointer on the object.

So, we have developed a *surface cursor*: once an object is selected, the cursor moves continuously on the surface in the direction of the virtual hand. The displacement vector of the tracker, defined by two successive positions is mapped into a displacement on the surface. The surface cursor is really tridimensional as the user is able to move on the whole surface: in particular, he can pick points that are hidden from the user with a surrounding gesture. Furthermore, by changing scale between the movements of the real hand and the virtual hand, the surface cursor is precise. In conclusion, the surface cursor keeps the swiftness and the precision of the mouse but in three dimensions.

### 3.3 Surgery simulation

At the beginning of the simulation, the user displays the surfaces of the skull and the face of the patient extracted from CT-Scan, MRI or Cyberware. The example that is presented bellow shows a skull and a face model that do not originate from the same patient which explains the discrepancy of shape existing between both





Figure 8: The virtual hand is used for cutting and moving skull fragments

models. However, this example does correctly reflect the overall principle of the surgery simulator.

On both surfaces, the user defines the fat tissue by selecting with the mouse or the surface cursor the opposite regions to be connected. He then activates the tissue building procedure and enters few parameters (number of layers, stiffness coefficient) (see Figure 9). At the end, the tissue are smoothed to regularly fill the space between the two regions.

In order to cut skull fragments, the user draws a closed contour either along the continuous path of the surface cursor, or along segments joining points selected manually with the mouse. A contour is then created, splitting the object into two independent regions that retain their initial attributes. Cutting can be forbidden according to the object topology. Finally, with the virtual hand, the user moves the different skull fragments to modify the skull shape. Once the cutting process is completed, fat tissues deform the face according to the skull modifications. A rendered and texture-mapped image of the deformed face is displayed in figures 10 and 11

## 4 CONCLUSION AND FUTURE WORK

In this paper, we have demonstrated the potential of general modeling tools for surgery simulation. Surface and volumetric simplex meshes are well-suited to simulate the deformation of organic models of complex topology. We plan to introduce those deformable models into an abdominal videosurgery simulator.

Computer graphics and virtual reality techniques are essential to achieve realistic and intuitive surgery simulation. Full immersion of the surgeon in the virtual space is not necessary to perform craniofacial surgery and is currently impossible due to the limit of existing technologies. However, force and tactile feedback would greatly enhance the realism of the simulation.

In the future, we plan to improve our testbed and integrate some tools developed in the Epidaure project:

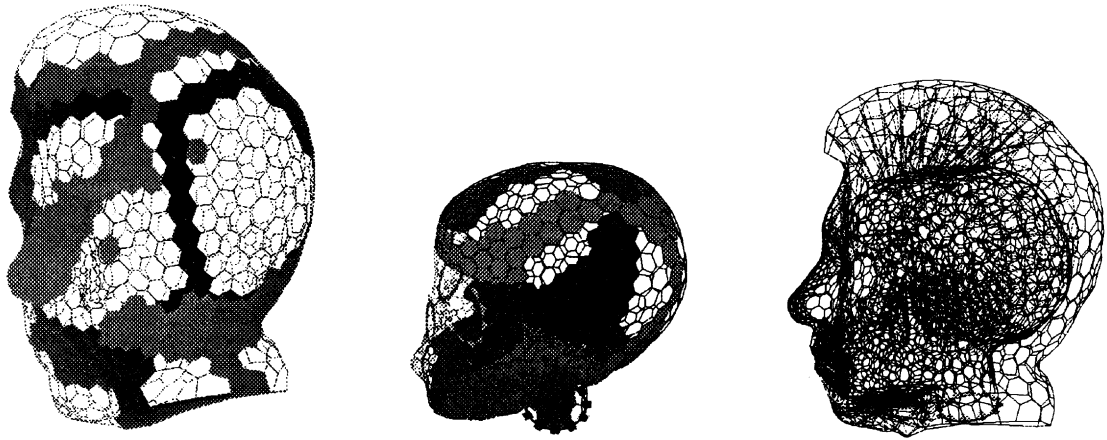


Figure 9: **Left and center** The corresponding regions on the two face and skull models that are connected with fat tissues; **Right** The fat tissue, face and skull models



Figure 10: Rendered face before and after surgery simulation



Figure 11: Textured face before and after surgery simulation

- Superposition of a abnormal skull with a healthy one or an anatomical atlas to help the physician during the simulation and to check results.<sup>15</sup>
- Automatic sorting for skull fragments with respect to geometrical criteria to provide an automatic skull reconstruction.
- Multimodality registration, for instance, to visualize the brain inside the skull in order to improve the realism of the simulation.

## ACKNOWLEDGMENTS

This work was funded in part by a grant from the **Digital Equipment Corporation**

## 5 REFERENCES

- [1] Michael Bajura, Henry Fuchs, and Ryutarou Ohbuchi. Merging virtual objects with the real world. *Computer Graphics*, 26(2):203–210, July 1992.
- [2] L.J. Brewster, S.S. Triveldi, H.K. Tuy, and J.K. Udupa. Interactive surgical planning. *IEEE Computer Graphics and Applications*, 4:31–40, 1984.
- [3] Ph. Cinquin. Gestes medico-chirurgicaux assistes par ordinateur. *Annales de Radiologie*, 36(6/7):386–406, 1993.

- [4] Court B. Cutting. Applications of computer graphics to the evaluation and treatment of major craniofacial malformations. In Jayaram K. Udupa and Herman Gabor T., editors, *3D Imaging in Medicine*, chapter 6, pages 163–189. CRC Press, 1991.
- [5] H. Delingette. Simplex meshes: a general representation for 3d shape reconstruction. Technical Report 2214, INRIA, March 1994.
- [6] H. Delingette, M. Hebert, and K. Ikeuchi. Shape representation and image segmentation using deformable surfaces. In *IEEE Computer Vision and Pattern Recognition (CVPR91)*, pages 467–472, June 1991.
- [7] H. Delingette, Y. Watanabe, and Y. Suenaga. Simplex based animation. In *Models and Techniques in Computer Animation (Computer Animation'93)*, 1993.
- [8] R. et al. Kikinis. Interactive visualization and manipulation of 3d reconstructions for the planning of surgical procedures. In *Visualization in Biomedical Computing*, pages 559–563. SPIE, 1992.
- [9] J.L. Marsh M. W. Vannier and J.O. Warren. Three dimensional computer graphics for craniofacial surgical planning and evaluation. In *Computer Graphics*, volume 17, pages 263–273, 1983.
- [10] Daniel Marchac and Dominique Renier. New aspects of craniofacial surgery. *World Journal of Surgery*, 14:725–732, 1990.
- [11] J. Marsh, M. Vannier, and R. Knapp. Computer assisted surface imaging for cranofacial deformities. In M. Hebal, editor, *Advances in Plastic and Reconstructive Surgery*. Year Book Medical Publishers, 1985.
- [12] Jun Satoh, Hiroaki Chiyokura, Masahiro Kobayashi, and Toyomi Fujino. Simulation of surgical operations based on solid modeling. In Toshiyasu L. Kunii, editor, *Visual Computing. Integration Computer Graphics with Computer Vision*, pages 907–916, Tokyo (Japan), 1992. Computer Graphics Society, Springer Verlag.
- [13] H. Taylor, R. Augmentation of human precision in computer-integrated surgery. In *Innovation et Technologie en Biologie et Medecine*, 1992.
- [14] D. Terzopoulos and Keith Waters. Physically-based facial modelling, analysis, and animation. *The Journal of Visualization and Computer Animation*, 1:73–80, March 1990.
- [15] J-P Thirion, O. Monga, Benayoun S., Gueziec A., and Ayache N. Automatic registration of 3d images using surface curvature. In *IEEE Int. Symp. on Optical Applied Science and Engineering*, San-Diego, July 1992.
- [16] M.L. Viaud. *Animation Faciale avec Rides d'expression*. PhD thesis, Universite Paris VI, 1992.
- [17] K. Waters. A physical model of facial tissue and muscle articulation derived from computer tomography data. In *Visualization in Biomedical Computing*, pages 574–583. SPIE, 1992.
- [18] Keith Waters. A muscle model for animating three-dimensional facial expression. *Computer Graphics*, 21(4), July 1987.
- [19] Takami Yasuda, Yasuhiro Hashimoto, Shigeki Yokoi, and Jun-Ichiro Toriwaki. Computer system for craniofacial surgical planning based on ct images. *IEEE Transactions on Medical Imaging*, 9(3):270–280, September 1990.